

A new morphology method for enhancing power quality monitoring system

Sen Ouyang ^{a,*}, Jianhua Wang ^b

^a College of Electric Power, South China University of Technology, Wushan Road, Guangzhou, Guangdong 510640, China

^b School of Electrical Engineering, Xi'an Jiaotong University, 28 West Xianning Road, Xi'an, Shaanxi 710049, China

Received 4 October 2004; accepted 2 June 2006

Abstract

By means of mathematical morphology (MM), power quality monitoring systems can detect disturbances very soon. However, the signal under investigation is often corrupted by noises, and the performance of the MM would be greatly degraded. This paper proposed a new fast approach to detection of transient disturbances in a noisy environment. In the proposed approach, the appropriate morphologic structure element, new proper combination of the erosion and the dilation morphologic operators can enhance the MM's capability. Furthermore, the soft-threshold de-noising method based on the wavelet transform (WT) was used for reference. In this way, the abilities of the MM can hence be restored. This method possesses the following advantages: high calculation speed, easy implementation of hardware and better use value. Finally, the validity of the proposed method is verified by the results of the simulation and the actual field tests.

© 2006 Elsevier Ltd. All rights reserved.

Keywords: Power quality; Mathematical morphology; Wavelet transform; Signal processing

1. Introduction

The electrical power quality (PQ) of power system has become an important issue for electric utilities and for their customers. Customers, in particular, have become less tolerant with power quality disturbances because these disturbances degrade the performance and efficiency of customer loads, especially power electronics loads. The common PQ signals people care about include voltage sag, swell, outage, flickers, frequency variation and so on. In order to determine the sources and causes of power quality, one must be able to detect and localize those disturbances and then classify their categories.

With the development of the WT technique, how to detect the power quality signals tends to be easy [1–5]. But this algorithm is so complicated that it is hard to work in many real-time field devices that are based on the com-

mon and cheap microprogrammed control unit (MCU), such as intelligent electrical apparatus. That is, calculation speed and de-noise capability of the signal processing method are all very important in the actual application. At this time, it is also hard to process all these PQ signals with the traditional tools or mathematical theories, such as WT, FFT and so on. In this paper, a new fast processing method (NFMM) based on the MM theory combined with threshold theory is proposed to de-noise and locate the disturbance of the power quality signals corrupted by noise. Since the MM method is very simple, it can be processed very fast, and the MM method is well fit for the non-linear signal processing problems [6], and different than the linear methods, such as FFT, WT and so on.

However, the MM still has its inherent disadvantage, like the wavelet method has. From an application-oriented point of view, the PQ signals under investigation are often corrupted by noise, and these kind of signals would degrade the effect of MM or WT method, or even lead to a wrong judgement [8,9]. This will be discussed in Section 2.

* Corresponding author. Tel.: +86 20 88370417; fax: +86 20 87110613.
E-mail address: ouyangs@scut.edu.cn (S. Ouyang).

To enhance the de-noise capability and calculation speed of NFMM, some points are discussed in this paper. These points include the appropriate morphologic structure element, combination mode of the erosion and the dilation morphologic operators.

Since Professor Donoho proposed the soft-threshold algorithm [7] in 1994, the wavelet de-noising technique based on the soft-threshold and other threshold algorithms had been well used in signal processing [8–10]. Then the combination of the MM and the threshold algorithm is discussed in this paper. In this way, the NFMM, which is different from the tradition processing method, can carry out the de-noising and disturbance location task better.

Furthermore, the aim of this paper's work is to form a new, effective and fast method, which can be real-time executed in the common and cheap MCU chip. So the compact design of NFMM is very necessary. This is also discussed in this paper.

At last, the theory analysis, calculation time and efficiency are given, and the validity of the proposed method is verified by the results of the simulation. The proposed method is simple, fast, effective, and a practical way to practice.

This paper is organized as follows. In Section 2, the theory of MM and the point of its structure element are introduced, the NFMM is mentioned in Section 3. The calculation speed, hardware resource demand, the sampling rate demand and the simulation and actual field data results are all presented in Section 4, and the de-noise capability and results are presented in Section 5.

2. Theory of mathematical morphology

2.1. Basic theory

The theory of MM was proposed to deal with the image [11–13]. With development, MM, which is based on the set operations, provides an approach to the development of non-linear signal processing operators that incorporate shape information of a signal. In MM operations, the result of a set transformed by other sets depends on the shapes of the two sets involved. The shape of a signal is determined by the values that the signal takes on. The shape information of the signal is extracted by using a structure element to operate on the signal.

The basic operators of MM are dilation and erosion, and the other morphology operators, such as opening and closing, can be derived from these two operators. And the morphologic structure element is another kind of set, with which the morphology operation can deal with an object. Always, the structure element is small than the object set, and is set up according to the figure character of the object set.

Consider a binary image as a set A in 2-D Euclidean space E^2 . Let the compact set $B \in E^2$ denote the structure element, which usually has a simple shape, and $B = \{-b \mid b \in B\}$ denotes the symmetric set of B with

respect to the origin, and \emptyset denotes the empty set. The translation of A by a point $z \in E^2$ is denoted by A_z and defined as $A_z = \{x + z \mid x \in A\}$. Then, the basic binary can be defined as follows [14]:

$$A \oplus B = \bigcup_{b \in B} A_b = \left\{ z \mid \bigvee_{b \in B} B_z \cap A \neq \emptyset \right\} \quad (1)$$

$$A \ominus B = \bigcap_{b \in B} A_{-b} = \{z \mid B_z \subseteq A\} \quad (2)$$

where \oplus denotes the dilation, and \ominus denotes the erosion.

Since the signals of power system are 1-D. There are different changes with Eqs. (1) and (2). Let x be a 1-D signal, and B be the structure element (a 1-D set). Where H and K are their regions respectively $H = \{1, 2, \dots, N\}$, $K = \{1, 2, \dots, M\}$, and $M < N$. M and N are integers. Then the dilation of the discrete signals $x(n)$ ($n \in H$) is

$$(x \oplus B)(n) = \text{Max}_{p=n-M+1, \dots, n} \{x(p) + B(n-p)\}, \\ \{n = M-1, M, \dots, N-1\} \quad (3)$$

where p is a integer.

And the erosion operation is

$$(x \ominus B)(n) = \text{Min}_{v=0, \dots, M-1} \{x(n+v) - B(v)\}, \\ \{n = 0, 1, \dots, N-M\} \quad (4)$$

where v is a integer.

Opening and closing are two derived operations defined in terms of erosion and dilation. According to Eqs. (3) and (4), the opening and closing operations are defined as

$$x \circ B = x \ominus B \oplus B \quad (5)$$

$$x \bullet B = x \oplus B \ominus B \quad (6)$$

where \circ denotes the opening operation, and \bullet denotes the closing operation.

The combination of the morphology operation can form morphology filters with different modes, such as the common filters: open-closing and close-opening filters [6,11–14]:

$$x \circ B = x \circ B \bullet B \quad (7)$$

$$x \odot B = x \bullet B \circ B \quad (8)$$

where \circ denotes the open-closing filter, and \odot denotes the close-opening filter.

2.2. Structure element

Besides the combination mode of the morphology operators, the structure element is very important and can also consumedly affect the processing result [6]. The common structure element has many kinds of shapes, such as bee-line, curve, triangle, circle and other polygons (such as diamond-shaped, hexagonal and so on) [6,11–14]. Non-close element is appropriate to the 1-D signals.

Moreover, the width or length of the structure element is under consideration. The longer, and more complex the

structure element, more the time taken to finish the morphology process. Take the line structure element for example, the longer the element, the better low-pass capability it has. That means better de-noising capability in some cases. According to the characteristic of the short-term PQ signals, a line element is chosen, which length is 3 and angle is zero in this paper.

3. The proposed method

3.1. Traditional method

Let the sampled signal be f . And the morphology results f_D , f_E , f_{OC} and f_{CO} can be obtained by using the dilation, erosion, open-closing and close-opening operations, respectively, according to Eqs. (3), (4), (7) and (8).

The traditional morphology de-noising scheme is usually defined in this way [6,15]:

$$f_{\text{de-noise}} = (f_{OC} + f_{CO})/2 \quad (9)$$

Let f_{WT} be the WT result of f . The comparison between MM and WT can denote their time–frequency characteristic, de-noising capability and so on. One voltage outage signal and its MM results and WT results are shown in Fig. 1.

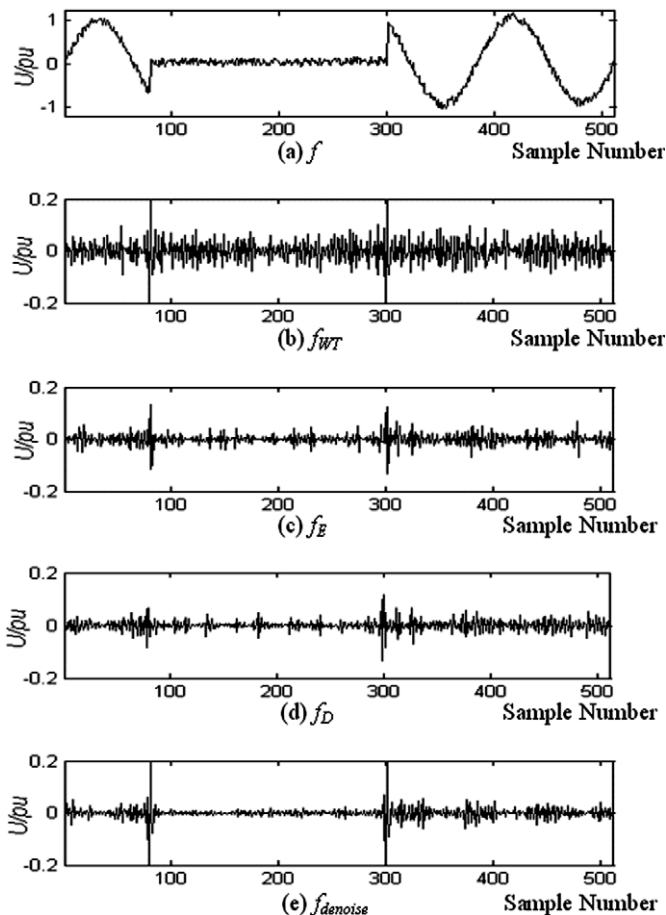


Fig. 1. The WT and MM processing results of the voltage outage.

As in Fig. 1, $f_{\text{de-noise}}$ can de-noise the sampled signal effectively, and retain the local characteristic at the same time. Comparing with $f_{\text{de-noise}}$, f_E and f_D have very little capability. Any way, both the WT and MM results are not so perfect, even MM method can work more perfectly. And these results all need to be de-noised and processed again. This is why the soft-threshold method [7] and other threshold methods [8–10] are developed with WT technology.

Since the soft-threshold algorithm first proposed by Professor Donoho [7], more were recently reviewed and enhanced by others [8–10]. The theory of soft-threshold is based on the different characteristics between the continuous signals and noises in the wavelet decompose process, and the statistics characteristic of the noises. With this theory, an alterable threshold can be designed to clear up most of the noises. And the threshold method can work well, and was adopted in this paper to enhance the capability of the proposed method. The effect of the soft-threshold method based WT can be found in Figs. 4–7 in this paper.

3.2. Design of the proposed algorithm

The destination of the de-noising method is to locate the disturbance from the signals corrupted by noise very soon. The proposed algorithm uses a simple combination of the morphology operators – just the dilation and erosion operators, and this can help to predigest the whole algorithm and reduce the calculation resource. Others, the soft-threshold method was inducted to do the re-denoise job, and this can help to detect the disturbance of the PQ signals.

Let the sampled sequence be $f(n)$, where $n = 1, 2, \dots, N$, n and N are integers. Then the length of $f(n)$ is N . The new algorithm includes the following steps:

1. First de-noise and location According to Section 2, the dilation result $f_D(n)$, and erosion results $f_E(n)$ can be obtained according to Eqs. (3) and (4) respectively, and let:

$$f_L(n) = f_D(n) - f_E(n) \quad (10)$$

where $f_L(n)$ is a temporary variable.

2. Noise intension calculation [7]

$$\sigma = \left(\sum_{n=1}^N |f_L(n)|/N \right) / 0.6745 \quad (11)$$

3. De-noise and location

$$f_M(n) = \begin{cases} 0 & f_L(n) \leq \sigma \\ f_L(n) - \sigma & f_L(n) > \sigma \end{cases} \quad (12)$$

where $f_M(n)$ is the morphology processing results.

The disturbance can be detected according to the calculation result $f_M(n)$. Furthermore, other compact threshold would be introduced in the following partition.

3.3. Experience formula

To speed up step 2 of the proposed algorithm, let

$$\sigma_j = \text{Max}(|f_L(n)|) \tag{13}$$

where σ_j is the experience threshold. And σ_j can use other appropriate experiential threshold or calculation results.

Then let

$$\sigma = (1 - u) \times \sigma_j \tag{14}$$

where $u \in [0, 1]$, and it was set to 0.9 in this paper. Here, σ is the de-noise threshold but not the noise intension.

If the signals under investigations are well known or there are enough apriority information, Eqs. (13) and (14) can work well. Otherwise Eq. (11) must be used.

3.4. Theory analyses of the proposed algorithm

According to the definition of the dilation, specially the 1-D definition, the dilation operation can shift and smooth the signal, fill the valley, but the aiguille can be kept. Moreover, the erosion operation can smooth the signal, and whittle the aiguille, but retain the valley of the signal. All these are shown in Figs. 2 and 3.

The qualitative analysis of these results is mentioned as follows. Let the signal be

$$f(n) = s + \delta + N_p + N_m \tag{15}$$

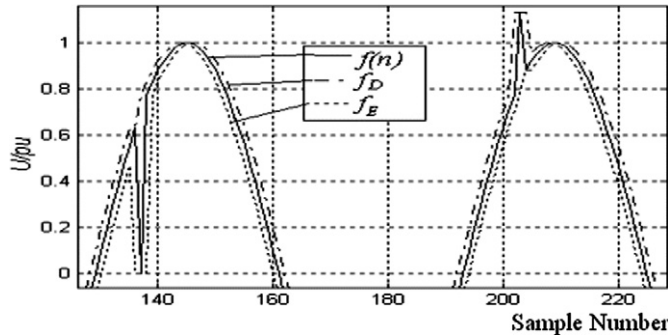


Fig. 2. The erosion and dilation results of the signal without noise.

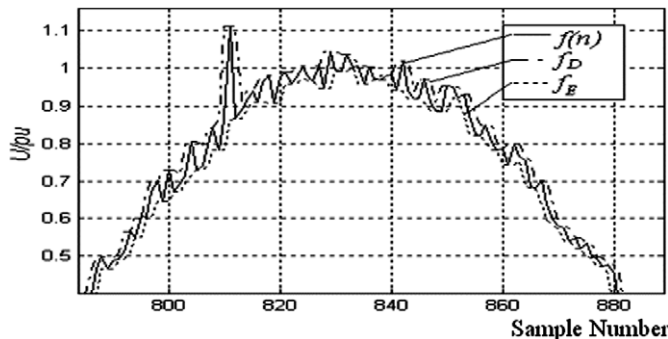


Fig. 3. The erosion and dilation results of the signal with noise.

where s is the signal without noise, δ is all the impactful disturbance signals, N_p is the noise which shape is like the wave aiguille, N_m is the noise which shape is like the wave valley.

After the erosion operation (only the erosion operation), the original signal $f(n)$ would be translated to some extent as in Fig. 2. And the valley part of the original signal can be kept when the noise is smoothed. These can be found in Figs. 1 and 3. Then

$$f_E \approx (s - z) + \delta_m + N'_m \tag{16}$$

where δ_m is the valley part of δ , z is the translation result according to the structure element, N'_m is the trough noise which was de-noised.

In the same way, after the dilation operation, original signal $f(n)$ can get

$$f_D \approx (s + z) + \delta_p + N'_p \tag{17}$$

where δ_p is the crest part of δ , N'_p is crest noise which was de-noised.

Then Eq. (10) can be turned into

$$f_L = f_D - f_E \approx 2z + \delta_p - \delta_m + N'_p - N'_m \tag{18}$$

According to the above mentioned information, $(\delta_p - \delta_m)$ must be plus, keeping the aiguille part disturbance, and turning the valley part disturbance over at the same time. In this way, all the disturbance parts can be kept. In the same way, the noise part gets the same result, except some was eliminated (as in Fig. 1). Expression (18) denotes that the calculation result can intensify the disturbance part, and restrain the noise part. And the calculation result must be plus and is translated up to some extent (according to the $2z$ weight).

It must be pointed out that expressions (16)–(18) are not tenable austerely. Because of the transform result it has some local distortion except the translation after the dilation and erosion operations. This is why expressions (16)–(18) do not get the equal sign. But these cannot change the theory analysis of above mentioned.

Finally, de-noising the transform result according to expression (18) can locate the disturbance. By this way, the opening and closing operations can also get the same or better results, but they will take more time.

4. Capability analysis and results

As a de-noise approach, what people care about includes: the de-noise capability, efficiency (calculation speed and the hardware resource demand), sampling rate demand and so on. The de-noise capability of NFMM will be discussed in Section 5, and the other capability of NFMM will be discussed in this section.

Let the simulation signal be f_s , and f denote the result of f_s which is corrupted by noise. f_{WT} is the WT operation result of f , and f_{STWT} is the soft-threshold WT (STWT) [7] operation result of f . According to Eqs. (10)–(12), f_L and

f_M are the morphology operation results of f . The comparison of f_M and f_{STWT} can indicate the capability of the proposed method.

4.1. Theory and actual efficiency analysis

As a signal processing method, the very little hardware resource demand and the faster calculation speed are more satisfactory and when applied it can attain the same or better results. As a comparison, the efficiency of the NFMM, FFT and WT should be given in this section. Let the length of the sampled data be N , and the length of the structure element be K . In the erosion process, there would be $K(N - K)$ comparison operation process and $K(N - K)$ minus operation process. The time that the compare operation process takes is about double than that the minus or plus operation process takes – it depends on the actual MCU chip, such as MCS 196, MCS 51, DSP and so on. Anyway, the erosion process will take (convert to the plus operation times)

$$T_M = 3 \times K \times (N - K) \tag{19}$$

As is well known the operation times of FFT are [17]

$$T_{FFT} = (N \log_2 N) / 2 \tag{20}$$

Let the decompose layer of WT be M , and the length of the wavelet filter be L . Then the operation times of wavelet decompose is [18]

$$T_{WT} = 4(L + 1)(N + ML - 2L + M) \tag{21}$$

From the theory analysis, it can be found that the calculation time of NFMM T_M is the most small, and $T_{FFT} < T_{WT}$.

All the above are the theory and part of the calculation times. The actual process has some difference. Let M be 5, and the wavelet be Db4, which $L = 8$. The simulation environment is Matlab. Then the calculation results can be obtained, and are shown in Table 1. And the comparing results are the same with the theory analysis.

Actually, even the evaluate operation (such as the assemble program $AX = 0 \times 10$, in MCS 196) will take a half plus period, maybe there are some differences with each kind of MCU chip. And large numbers of calculation will lead to the frequent operation of the RAM and other registers in MCU, and the time to read or write different memory devices is totally different. Furthermore, the exec-

Table 1
Simulation calculation time of each method

N	Calculation time (ms)		
	FFT	NFMM	WT
64	20	10	50
128	50	20	85
256	–	–	135
512	–	–	295

Table 2
Actual calculation time of each method

	Calculation time (ms)		
	DFT	FFT	NFMM
Device I	0.26	2.48	0.97
Device II	0.069	0.66	0.27

utive code and their executive efficiency are different according to different software’s compilation and translation environments. All in all, the actual executive efficiency is more complex than Eqs. (19)–(21).

There are two kinds of self-designed intelligent devices to test the actual calculation speed of the algorithms, including DFT, FFT and NFMM. Device I is a over-current protection unit, which is based on the MSP430F149C chip (work in 16 MHz). And device II is a PQ monitor device, which is based on the DSPF2407 chip (work in 30MIPS). The DFT, FFT and NFMM are carried out in these devices, and all are programmed based on ANSI C. Let the sampling rate be 16 points/period, and the length of the sampled data be 16, then the comparison can be obtained as shown in Table 2. Then comparing with other signal processing methods, the speed superiority of the NFMM is validated by the simulation results in Table 1 and actual data results in Table 2.

4.2. Other capabilities

Except for the efficiency, the NFMM is effective with low sampling rate. The WT method needs high sampling

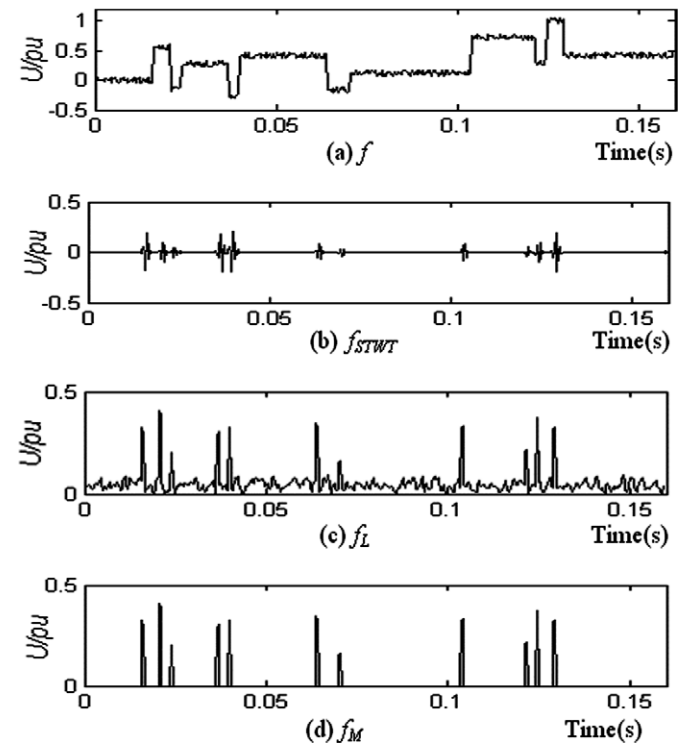


Fig. 4. The processing results of the Blocks signal when the sampling rate is 3.2 kHz.

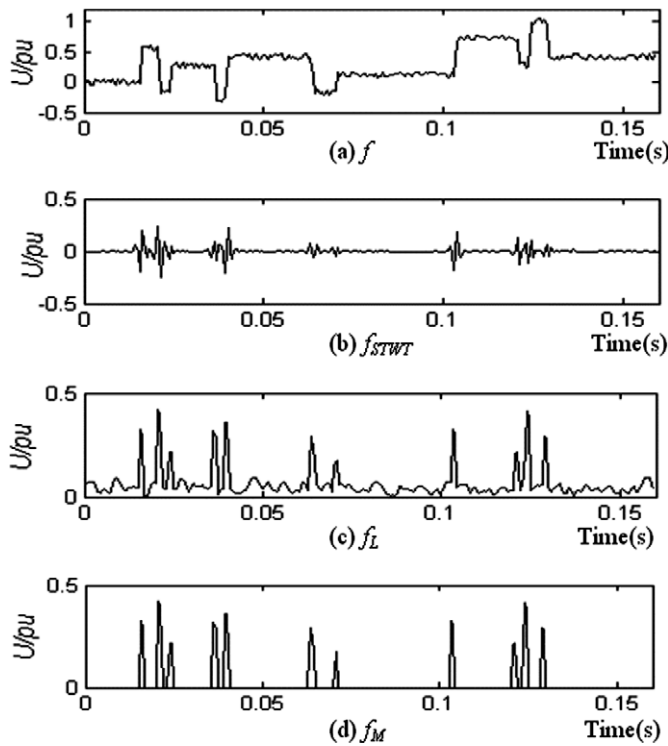


Fig. 5. The processing results of the Blocks signal when the sampling rate is 1.6 kHz.

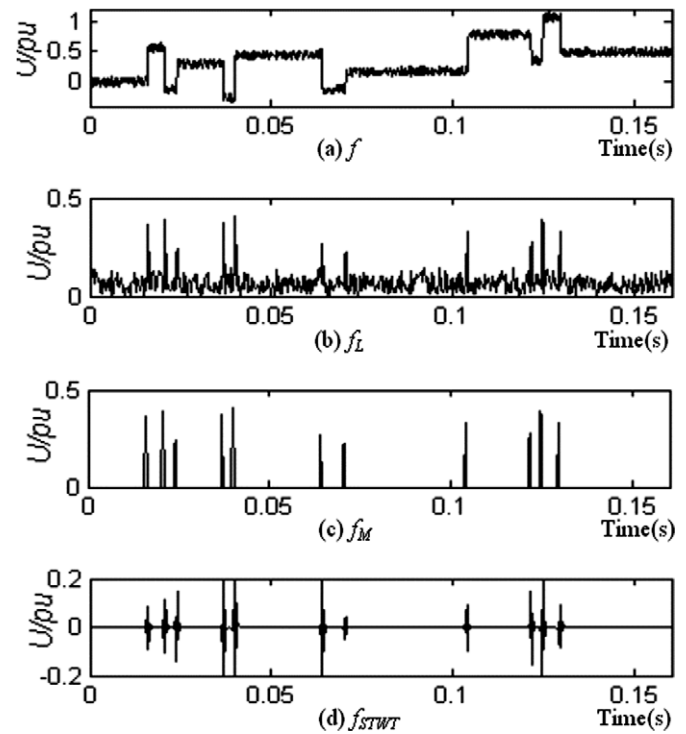


Fig. 6. The processing results of the Blocks signal.

rate or its capability would be weakened (STWT is based on WT). And this is one of the reasons why WT needs so many calculation resources. The WT method needs 6.4 kHz (128 points/period) or higher sampling rate, while the NFMM only needs 1.6 kHz or 800 Hz (it is a common and very low sampling rate). And this is helpful to speed up the processing process. Also, a comparison is shown in Figs. 4 and 5.

As in Fig. 4, both NFMM and STWT can all detect the disturbance. But comparing with Fig. 5 (this figure will be illustrated in Section 5), in the result of WT (Figs. 4(b) and 6(d)), some confusion is present. That is because of the lower sampling rate. Moreover, the result of WT becomes more promiscuous when the sampling rate was reduced to 1.6 kHz, as in Fig. 5(b). And this result is so unclear as to lead to wrong judgements. At the same time, the results of NFMM can at the time keep be clear as to distinguish all the disturbances, even the sampling rate was reduced to 1.6 kHz. This speciality can be very helpful to the hardware design.

5. De-noise capability and results

This section will give the de-noise results of the simulation and actual data.

5.1. Simulation

The simulation signals include the Blocks, and voltage sag, notch and so on. The sampling rate is 6.4 kHz (128

points per period). And some noises were added into these signals to verify the proposed algorithm.

The signal Blocks are commonly used to test the capability of the de-noising method. The processing results of the Blocks are showed in Fig. 6. As in Fig. 6, the morphology results still retain some noise (as shown in Fig. 6(a)), but the result according to Eq. (11) can exactly detect and locate the disturbance, which de-noising and location capability is more perfect than soft-threshold WT method. And the comparison of Fig. 6(d) and 1(b) can tell that the soft-threshold method can work.

By the way, f_L has an up translation relative to f_M . This can be explained by expression (18).

And the processing results of the voltage notch are shown in Fig. 7. And the same conclusion can be obtained.

5.2. Noise tolerance testing

To test the ability of the NFMM in tolerating the noise on the input signals, different levels of noise with the signal noise ratio (SNR) values ranging from 50 to 30 dB were used. The value of the SNR is defined in:

$$Q_{\text{SNR}} = 10 \ln(P_S/P_N) \quad (22)$$

where P_S is the variance (power) of the signal, and P_N is that of the noise.

The simulation signals include voltage sag, swell and notch. And these signals accord with Standard IEEE 1159 [16]. The sampling rate is 6.4 kHz. The added noises are white noise. Then the comparison of the detection

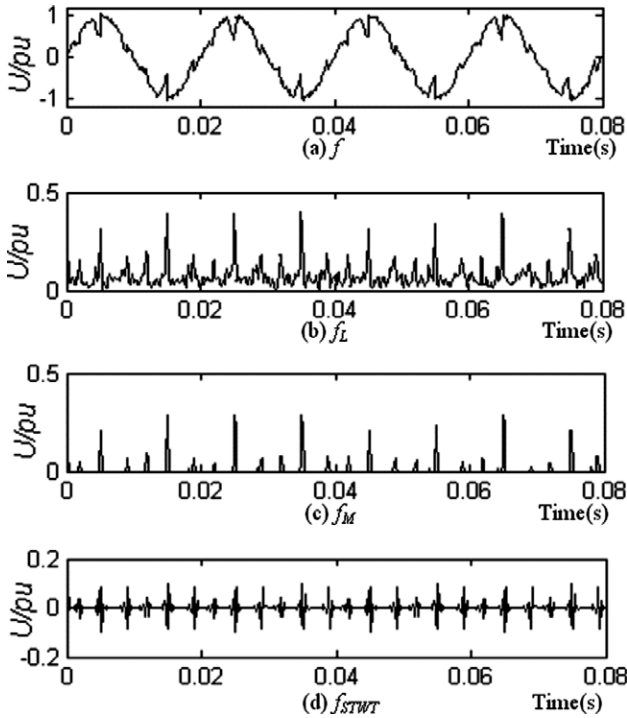


Fig. 7. The processing results of the voltage notch.

rate between NFMM and STWT are shown in Table 3. As in Table 3, the tolerance of the both the methods declines as the SNR becomes smaller, but the proposed method is more sensitive, and it cannot work so perfect as the STWT do, specially in the very strong noise environment. But when the SNR is greater than 35 dB, the NFMM retains the essential capability, comparing with STWT.

Table 3

Detection rate (%) of different disturbances and levels of noise added

SNR (dB)	Sag		Swell		Notch	
	NFMM	STWT	NFMM	STWT	NFMM	STWT
50	100	100	100	100	100	100
45	98	96	93	94	93	91
40	85	86	82	84	85	86
35	71	78	72	73	62	69
30	57	69	55	65	38	46

5.3. Actual field data results

To validate the capability of the NFMM more realistically, some field data were derived from a 220 V-level power system (50 Hz) of a laboratory, where there are many electrical and electronic devices working. And some intelligent devices (self-design) are used to sample and calculate the sampled data. All these devices are under a field environment. Then, the sampled dates are send to a PC and are calculated with WT or NFMM method, and all these results are shown with the self-design software. And a special PQ testing device ONLLY 6108G was used to carry out the experiment at the same time. This device can create some PQ signals (voltage and current), such as normal, interruption, harmonic, sag, swell and so on. These are helpful to validate the NFMM and to design the self-design devices.

A transient sampled signal and its processing result are shown in Fig. 8. As in Fig. 8, the upper part is the original data of the sampled signal, the middle part is the sampled signal's waveform, and the bottom part is the processing result using NFMM.

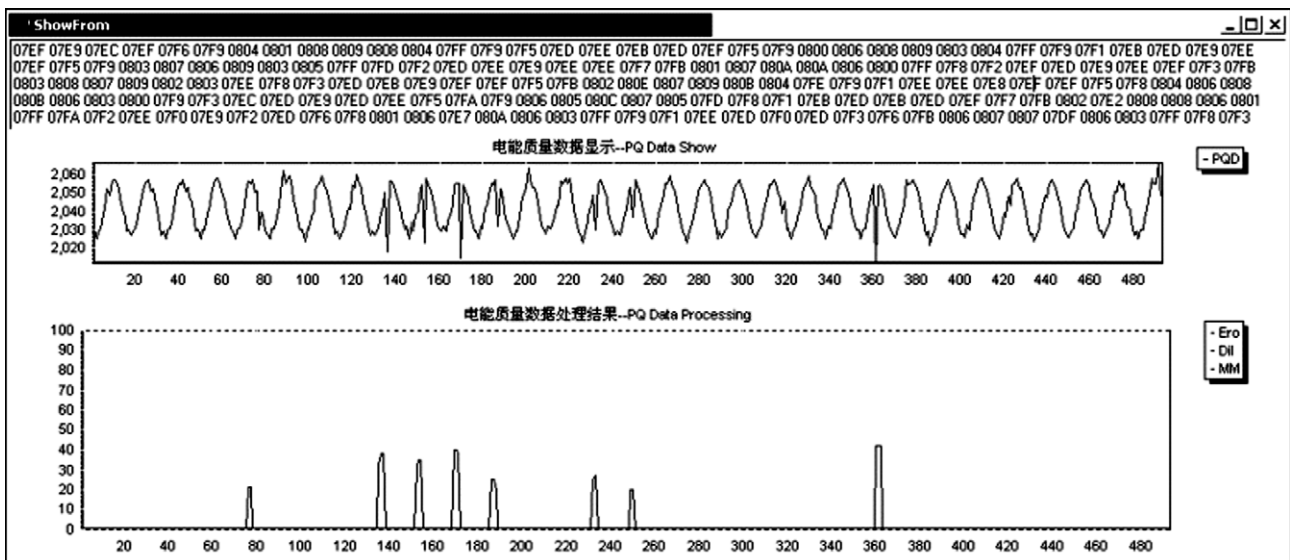


Fig. 8. The processing results of the field transient voltage signal.

6. Conclusion

To enhance the capability of the PQ signal processing method in a noisy environment, and to speed up the process enough to be real-time executed by the common and cheap MCU, a new fast morphology method has been proposed and integrated with the soft-threshold theory in this paper. By adopting the appropriate morphologic structure element, and proper combination of the erosion and the dilation morphologic operators, a simple morphology processing is formed. Furthermore, the threshold theory can help to enhance the whole method. Extensive tests using diverse data for simulated signals and field dates show that the NFMM can works effectively. Moreover, the fast capability of NFMM is validated by the actual devices based the cheap MCU chip, including MSP430, DSPF2407 and so on. Although the capability of NFMM is not so better than that of WT in high sampling rate, this method can still work in low sampling rate. All of the above prove that the proposed method is simple, fast, effective, and a practical way to practice.

Acknowledgements

The authors wish to acknowledge the financial support by the National Ministry of Education of China for this project, under the National High-Tech Industry Development Project, No. 1883.

The project was also Supported by the Key Projects of National Natural Science Foundation of China, No. 50337010.

References

- [1] Robertson C, Camps OI, Mayer JS, Gish WB. Wavelet and electromagnetic power system transients. *IEEE Trans Power Deliver* 1996;11(2):1050–8.
- [2] Santoso S, Grady WM, Lamoree J, Bhatt SC. Characterization of distribution power quality events with Fourier and wavelet transforms. *IEEE Trans Power Deliver* 2000;15(1):247–54.
- [3] Gaouda AM, Salama MA, Sutan MR, Chikhani AY. Power quality detection and classification using wavelet-multiresolution signal decomposition. *IEEE Trans Power Deliver* 1999;14(4):1469–76.
- [4] Santoso S, Powers EJ, Grady WM, Parsons AC. Power quality disturbance waveform recognition using wavelet-based neural classifier, Part1: Theoretical foundation, Part2: Application. *IEEE Trans Power Deliver* 2000;15(1):222–35.
- [5] Angrisani L, Daponte P, Apuzzo D, Testa A. A measurement method based on the wavelet transform for power quality analysis. *IEEE Trans Power Deliver* 1998;13(4):990–8.
- [6] Serra J. *Image analysis and mathematical morphology*. New York: Academic; 1982.
- [7] Donoho DL. De-noising by soft-thresholding. *IEEE Trans Inf Theory* 1995;41(3):613–27.
- [8] Downie R, Silverman W. The discrete multiple wavelet transform and thresholding methods. *IEEE Trans Signal Process* 1998;46(9):2558–61.
- [9] Hilton L, Ogden T. Data analytic wavelet threshold selection in 2-D signal denoising. *IEEE Trans Signal Process* 1997;45(2):496–500.
- [10] Carl T. The what, how, and why of wavelet shrinkage denoising. *Comput Sci Eng* 2000;2(3):12–9.
- [11] Zana F, Klein JC. Segmentation of vessel-like patterns using mathematical morphology and curvature evaluation. *IEEE Trans Image Process* 2001;10(7):1010–9.
- [12] Chatzis V, Pitas I. A generalized fuzzy mathematical morphology and its application in robust 2-D and 3-D object representation. *IEEE Trans Image Process* 2000;9(10):1798–810.
- [13] Maragos P. Differential morphology multiscale image dynamics, max–min difference equations, and slope transforms. *IEEE Int Conf Image Process, ICIP* 1994;2:545–9.
- [14] Maragos P. A representation theory for morphological image and signal processing. *IEEE Trans Pattern Anal Machine Intell* 1989;11(6):586–99.
- [15] Chu C-HH, Delp EJ. Impulsive noise suppression and background normalization of electrocardiogram signals using morphological operators. *IEEE Trans Biomed Eng* 1989;36(2):262–73.
- [16] IEEE recommended practice for monitoring electric power quality. *IEEE Std 1159-1995*, IEEE, New York, NY, 1995.
- [17] Stanley WD, Dougherty GR, Dougherty R. *Digital signal processing*. Reston, VA: Reston Publishing Co.; 1984.
- [18] Cheng ZX. *Wavelet analyse algorithm and its application*. Xi'an, China: Xi'an Jiaotong University Press; 1998.